Environmental Science & Technology

Article

Cite This: Environ. Sci. Technol. 2018, 52, 6714−6722

pubs.acs.org/est

Trace Metals in Soot and $PM_{2.5}$ from Heavy-Fuel-Oil Combustion in a Marine Engine

J. C. Corbin,[†,‡] A. A. Mensah,[¶] S. M. Pieber,[†] J. Orasche,[§,∥] B. Michalke,[⊥] M. Zanatta,[†,#] H. Czech,[∥] D. Massabò,[◆,○] F. Buatier de Mongeot,[○] C. Mennucci,[○] I. El Haddad,[†] N. K. Kumar,[†] B. Stengel,[▽,□] Y. Huang,[∥] R. Zimmermann,[∥,§,□] A. S. H. Prévôt,[†] and M. Gysel*[,†]

[†]Laboratory of Atmospheric Chemistry, Paul Scherrer Institute, CH-5232 Villigen, Switzerland

[¶]Institute for Atmospheric Chemistry, ETH Zurich, 8092 Zurich, Switzerland

[§]Joint Mass Spectrometry Centre, Cooperation Group Comprehensive Molecular Analytics, Helmholtz Zentrum München, Ingolstädter Landstrasse 1, 85764 Neuherberg, Germany

[∥]Joint Mass Spectrometry Centre, Chair of Analytical Chemistry, Institute of Chemistry, University of Rostock, Dr.-Lorenz-Weg 2, 18059 Rostock, Germany

[⊥]Research Unit Analytical Biogeochemistry, Helmholtz Zentrum München, 85764 Neuherberg, Germany

[◆]INFN, Sezione di Genova, Via Dodecaneso 22, 16146 Genova, Italy

[○]Department of Physics, University of Genoa, Via Dodecaneso 33, 16146 Genova, Italy

[▽]Department of Piston Machines and Internal Combustion Engines, University of Rostock, Albert-Einstein-Strasse 2, 18059 Rostock, Germany

[□]HICE − Helmholtz Virtual Institute of Complex Molecular Systems in Environmental Health, 85764 Neuherberg, Germany

Supporting Information

ABSTRACT: Heavy fuel oil (HFO) particulate matter (PM) emitted by marine engines is known to contain toxic heavy metals, including vanadium (V) and nickel (Ni). The toxicity of such metals will depend on the their chemical state, size distribution, and mixing state. Using online soot-particle aerosol mass spectrometry (SP-AMS), we quantified the mass of five metals (V, Ni, Fe, Na, and Ba) in HFO-PM soot particles produced by a marine diesel research engine. The in-soot metal concentrations were compared to in-$PM_{2.5}$ measurements by inductively coupled plasma-optical emission spectroscopy (ICP-OES). We found that <3% of total $PM_{2.5}$ metals was associated with soot particles, which may still be sufficient to influence in-cylinder soot burnout rates. Since these metals were most likely present as oxides, whereas studies on lower-temperature boilers report a predominance of sulfates, this result implies that the toxicity of HFO PM depends on its combustion conditions. Finally, we observed a 4-to-25-fold enhancement in the ratio V:Ni in soot particles versus $PM_{2.5}$, indicating an enrichment of V in soot due to its lower nucleation/condensation temperature. As this enrichment mechanism is not dependent on soot formation, V is expected to be generally enriched within smaller HFO-PM particles from marine engines, enhancing its toxicity.

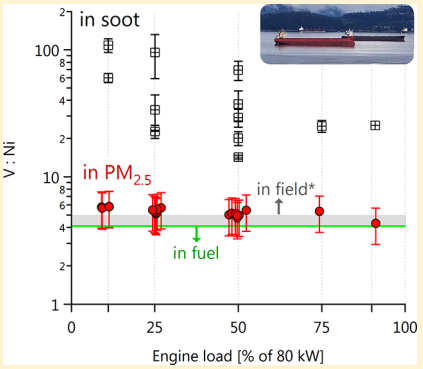

INTRODUCTION

Marine engines represent a major source of atmospheric particulate matter (PM), with global emissions comparable to road traffic and aviation.[1] As close to 70% of shipping emissions occur within 400 km of coastlines,[2] and marine-engine PM may contribute significantly to local mortality.[3] The remaining 30% of emissions are the major source of anthropogenic air pollution in the marine environment.

Ocean-going marine engines typically operate on the cheap residual fuel known as Heavy Fuel Oil (HFO). Due to its high sulfur content, HFO has already been prohibited within the so-called Sulfur Emission Control Areas (SECAs, coastal zones near Europe and North America). However, as ∼80% of global shipping in 2015 originated from ports outside of SECAs,[4] large urban populations remain exposed to significant levels of HFO exhaust.[5−7]

Epidemiological studies have suggested a connection between HFO-combustion PM and mortality[8] as well as morbidity.[9] Multiple toxic species are found in HFO; HFO PM is rich in transition metals and polycyclic aromatic hydrocarbons (PAHs), both of which play a role in its toxicity.[10−14] A significant mass fraction of these transition metals may be

Received: April 3, 2018
Accepted: April 24, 2018
Published: April 24, 2018

DOI: 10.1021/acs.est.8b01764
Environ. Sci. Technol. 2018, 52, 6714−6722

present in the smaller PM fractions,[15−19] such as $PM_{2.5}$ (PM with diameters <2.5 μm), which are small enough to penetrate to and affect the human bronchi and alveoli.[20] When insoluble, such particles may remain in the lungs for days,[21−24] catalyzing oxidative stress.[25] The even smaller $PM_{0.1}$ size fraction is more likely to pass through exhaust aftertreatment systems[26] and are small enough to enter the bloodstream after inhalation.[24] The passage of $PM_{0.1}$ through aftertreatment systems is particularly noteworthy, as such aftertreatment systems are required in SECAs when HFO is combusted.

The most abundant trace metal in HFO is vanadium(V), which is also particularly toxic.[27] Nickel (Ni) and other metals are present in smaller amounts. Such metals are typically present as oxides, though ∼10% exist as organometallic compounds.[28−30] Some fraction of these metallic compounds may vaporize during fuel combustion before nucleating into new particles.[18,31,32] These nucleated particles may then act as in-flame condensation nuclei for soot formation,[16,33] leading to metal or metal-oxide inclusions in soot with diameters of ∼5−10 nm.[34] These inclusions have the potential to influence soot emissions by catalyzing soot oxidation.[31,35,36] The inclusions may be composed of metal alloys or oxides, such as Ni, Ni_2Fe, Fe_2S, V_2O_3, and $Ni_3Fe_2O_3$.[33] Popovicheva et al.[33] identified these compounds in a ship-exhaust PM sample using scanning electron microscopy (SEM), which provided single-particle elemental as well as morphological information. However, only a limited number of particles can be analyzed quantitatively by SEM due to its labor intensity.

In contrast to SEM, online aerosol mass spectrometry provides the opportunity to quantify metals in aerosol particles with high throughput. The recently developed Soot-Particle Aerosol Mass Spectrometer (SP-AMS),[37] which uses a 1064 nm-laser vaporizer to specifically vaporize particles which absorb light efficiently at that wavelength, has the ability to selectively quantify metals in soot particles since few materials other than soot do so.[37−40] Here, we operated the SP-AMS laser vaporizer in tandem with the standard AMS thermal vaporizer[41] to obtain additional information about particle composition.

In this manuscript, we refer to the particles vaporized by the SP-AMS laser (and not the AMS thermal vaporizer) as soot particles. Since these particles have aerodynamic diameters in the range of 60 to 600 nm (discussed further below), soot particles are a subcategory of $PM_{2.5}$. A soot particle is a flame-synthesized particle primarily comprised of an aggregate of refractory black carbon (rBC) spherules, where rBC is the light-absorbing, insoluble, graphene-like PM that vaporizes at ∼4000 K.[42,43] It follows that soot may contain additional condensed material, such as sulfates and organics, as well as metal inclusions. We note that in the primary engine emissions studied here, the mass fraction of organics and sulfate internally mixed with soot was negligible,[44] so that the potentially ambiguous scenario of a particle containing only 10% rBC is irrelevant here. In HFO PM, a second type of rBC particle may be observed: char. Char particles are the supermicron, graphitized, often porous carbonaceous residues of fuel droplets.[16,32,33,45] Due to their different formation mechanisms, the trace-element composition of soot particles will be different than that of char particles. Crucially, the supermicron diameter range of char particles means that they are too large to be measured by the SP-AMS, so that SP-AMS measurements are intrinsically selective for soot particles, whereas filter samples may include both soot and char.

In this work, we present SP-AMS measurements of the internally mixed metal content of soot generated by a marine four-stroke diesel research engine operated on HFO. We use the term "metals" to describe the metal mass fraction of alloys, oxides, or other compounds. (Our observations indicate that metal alloys and/or oxides were the dominant species present in our sample.) The specific metals measured were vanadium, nickel, iron, sodium, and barium (V, Ni, Fe, Na, and Ba). In addition to the SP-AMS data, additional measurements of rBC mass concentration by laser-induced incandescence (single-particle soot photometer, SP2) and bulk $PM_{2.5}$ metal content by inductively coupled plasma-optical emission spectroscopy (ICP-OES) are presented. SEM measurements were performed to exclude the presence of char particles in our samples. Finally, measurements on two metal-free distillate fuels (marine gas oil, MGO, and diesel fuel) are used as controls.

MATERIALS AND METHODS

Experimental Section. The engine used in this study was a four-stroke, single-cylinder research engine installed at the Institute of Piston Machines and Internal Combustion Engines at the University of Rostock in Germany. The engine has a 150 mm bore and a 180 mm stroke and operates at a nominal 1500 rpm with a maximum power of 80 kW. The engine can be operated with both HFO and distillate fuels (here, MGO and diesel fuel, with diesel defined according to EN 590), and its layout represents a typical medium-speed large-bore engine. Further details are provided in Streibel et al.[34] Engines of these dimensions may be used on smaller ships as a main power supply, on large ships for ancillary power (at sea or while harbored), or as a backup power supply, e.g., in hospitals.

Aerosol samples from the engine exhaust were taken through an insulated sampling probe at 300 °C to a cyclone with a nominal cutoff diameter of 2.5 μm and then 10-fold diluted by a two-stage sampling system (Venacontra, DAS, Finland). The first dilution stage employed a porous-tube dilutor[46,47] in which compressed air flowed through pores in a cylindrical sampling volume to provide a sheath flow and minimize wall losses of vapors and particles. The second stage employed an ejector dilutor with a total flow rate of 150 L min^{-1}, which provides a good mixing of the sample with dilution air. Dilution ratios were calculated in real time from CO_2(g) measurements. Four parallel $PM_{2.5}$ filter samples were collected simultaneously with a modified speciation sampler (Rupprecht & Patashnik 2300, Thermo Scientific, Waltham, USA). The $PM_{2.5}$ samples were collected either on quartz-fiber filters (T293, Munktell, Sweden), PTFE membrane filters (PFF, Zefluor 1 μm, Pall, USA), or polycarbonate (Millipore, UK) with a flow rate of 10 normal liters per minute each. The quartz-fiber filters were conditioned before sampling by baking at 500 °C for at least 12 h. Filters were stored in sealed glass containers until sampling. Immediately after sampling, the filter samples were stored at −25 °C. Thermal/optical EC was determined with a DIR Model 2001a carbon analyzer according to the Improve A protocol.[48]

SP-AMS and SP2 (single particle soot photometer, described below) samples were taken following an additional 100-fold dilution relative to the filter samples, using two 10-fold ejector dilutors (PALAS GmbH, Germany). To allow a comparison between the real-time and filter-based measurements, real-time measurements were averaged over the filter sampling periods (typically 30 min), unless specified otherwise. Other real-time

DOI: 10.1021/acs.est.8b01764
Environ. Sci. Technol. 2018, 52, 6714−6722

measurements from these experiments are reported elsewhere.[44]

SEM was performed on HFO particles collected on polycarbonate filters (Millipore, UK) at a representative engine load of 50% load. A few nanometers of gold were deposited onto the filters to enhance sample conductivity prior to measurement with a Hitachi SU3500. The elemental composition of 56 particles was measured by Energy Dispersive X-ray spectroscopy (EDX) with the SEM. Simultaneous high-resolution images of the EDX-measured particles were not obtained. As these SEM-EDX measurements were performed as a supplement to the other measurements, they were much more limited in scope.

Inductively Coupled Plasma-Optical Emission Spectroscopy (ICP-OES). Inorganic elements were determined from PTFE filter samples using inductively coupled plasma-optical emission spectroscopy (ICP-OES, Spectro Ciros Vision, SPECTRO Analytical Instruments GmbH & Co. KG, Kleve, Germany). Each precisely weighed sample was added to a quartz vessel containing concentrated aqueous HNO_3 (analytical grade, Suprapur, Merck, Germany). The HNO_3 was sub-boiling distilled before use. The samples were then digested in a microwave digestion system (Paar GmbH, Germany) and diluted with deionized water (Milli-Q, Millipore, Germany) before measurement. The ICP-OES analytical procedure is described in full detail in the SI.

Single Particle Soot Photometer (SP2). A single particle soot photometer (SP2; Droplet Measurement Technologies, CO, USA) was employed to measure rBC mass concentrations by laser-induced incandescence[38,49] using a 1064 nm continuous-wave laser. Data were analyzed using the PSI SP2 Toolkit version 4.112. The SP2 quantitatively measures the rBC mass of single particles between ~0.7 fg (~80 nm rBC mass-equivalent diameter, d_{rBC}) and ~200 fg (~600 nm) with unit collection efficiency. Outside of this range, smaller particles are not detected; larger particles are still counted, but rBC mass is not quantified due to signal saturation. The rBC mass-equivalent diameter d_{rBC} was calculated according to a BC density of 1800 kg m^{-3}.[50] The SP2 was operated as described in Laborde et al.[51] Mass calibration was performed with nebulized reference rBC particles (fullerene-enriched soot, Alfa Aesar; stock 40971, lot FS12S011), which have been validated as a reference by Laborde et al.[52] The reference rBC particles were mass-classified (Aerosol Particle Mass analyzer model 3061, Kanomax) in order to determine a linear mass-response curve. The SP2 also measures particle scattering cross sections, which provides optical sizing of the particles (including non-rBC material); the scattering detectors were calibrated using 269 nm spherical polystyrene latex size standards.

Lognormal fits to the measured d_{rBC} size distributions were used to infer correction factors to account for unmeasured rBC mass in particles smaller or larger than the size-detection limits given above. An uncommonly large correction factor of 1.46 was obtained for HFO, due to the presence of a significant fraction of high-mass particles from residual fuel that saturated the detector of the SP2. This is discussed in detail in a separate manuscript[44] and is not relevant to this manuscript, considering the overall low in-soot metal concentrations reported here.

Soot-Particle Aerosol Mass Spectrometer (SP-AMS). The Soot-Particle Aerosol Mass Spectrometer (SP-AMS; Aerodyne Inc., USA) employs a 1064 nm, continuous-wave laser to vaporize rBC as well as internally mixed impurities.[37] The resulting vapor molecules are neutral,[53] except for those metals with exceptionally low ionization energies.[40,54] Vaporized species are analyzed by a high-resolution time-of-flight mass spectrometer after electron ionization.

The above-mentioned vaporization laser was alternately switched on and off, similarly to Corbin et al.[39] With the laser off, nonrefractory PM (nrPM) is flash vaporized on a 600 °C porous-tungsten vaporizer and subsequently analyzed similarly. These measurements are subsequently referred to as "AMS" measurements. The porous-tungsten vaporizer is also present in laser-on mode, in which case it vaporizes any nrPM which does not absorb sufficiently at 1064 nm, such as externally mixed OM or sulfate particles. The AMS measurements were used to obtain the reported OM concentrations, sulfate concentrations, and elemental ratios H:C and O:C following standard methods;[41,55−57] further details are provided in the SI. The ionization efficiency of the AMS (and SP-AMS) was calibrated using 300 nm mobility-diameter-selected ammonium nitrate (NH_4NO_3) particles.[41] The ionization efficiencies relative to nitrate (RIEs) used for OM and sulfate were 1.4 and 1.2, respectively.[58,59]

SP-AMS rBC mass concentrations $C_{rBC,SP\text{-}AMS}$ were quantified from the sum of carbon-cluster ions (C^+_{1-9}) using an RIE of 0.2.[37,39,60] We note that the ratio C^+_1:C^+_3 was unity for our samples, in contrast to the previously reported value[39] of 0.6 (Figure S1). $C_{rBC,SP\text{-}AMS}$ is proportional to the mass of rBC reaching the SP-AMS laser vaporizer, which must depend on the transmission efficiency E_z of particles from the SP-AMS aerodynamic lens to its laser vaporizer. E_z is a function of the particle free-molecular-regime aerodynamic diameter,[61] which is a function of the soot-aggregate monomer diameter, morphology, and internal mixing.[61−64] The reliable constraint of E_z for SP-AMS mass quantification is a topic of current research[63,64] and outside the scope of this work, as evaluated and discussed in the SI. Below, we therefore used the SP2-measured rBC mass concentrations $C_{rBC,SP2}$ to normalize $C_{rBC,SP\text{-}AMS}$ (eq 3) since the reliability of the SP2 in measuring rBC mass concentrations independently of mixing state has been thoroughly confirmed by previous studies.[52,65,66]

We quantified in-soot metal concentrations with the SP-AMS using the method recently demonstrated by Carbone et al.[40] That is, we used the RIEs reported by Carbone et al. to quantify the concentrations of V, Ni, Fe, Ba, and Na vaporized by the SP-AMS laser as $C_{M,SP\text{-}AMS}$. We note that the RIEs reported by Carbone et al. for Na and Ba (only) result in conservative lower-limit concentration estimates, as detailed in the SI. This does not apply to the concentrations reported for V, Ni, or Fe, for which quantification is accurate.

Each metal signal was quantified from the signal of its most abundant isotope. These isotopic signals were integrated to obtain peak areas, which were then divided by the relative abundance of that isotope to yield the total mass concentration $C_{M,SP\text{-}AMS}$ of that metal. A peak-specific SP-AMS limit of quantification of 20 ng m^{-3} was estimated for all metal ions via a novel procedure, described in the SI. Each relative abundance was directly measured and validated as consistent with literature. A small mass fraction of Fe (12%) and V (3.5%) was present as metal-oxide ions (MO^+_x); the mass of Fe or V in oxide ions was quantified and added to the corresponding mass of metal ions when reporting the mass concentrations of these species. The SI provides complete details on this novel procedure, as well as on the above-mentioned isotopic abundances and metal-oxide ions.

DOI: 10.1021/acs.est.8b01764
Environ. Sci. Technol. 2018, 52, 6714−6722

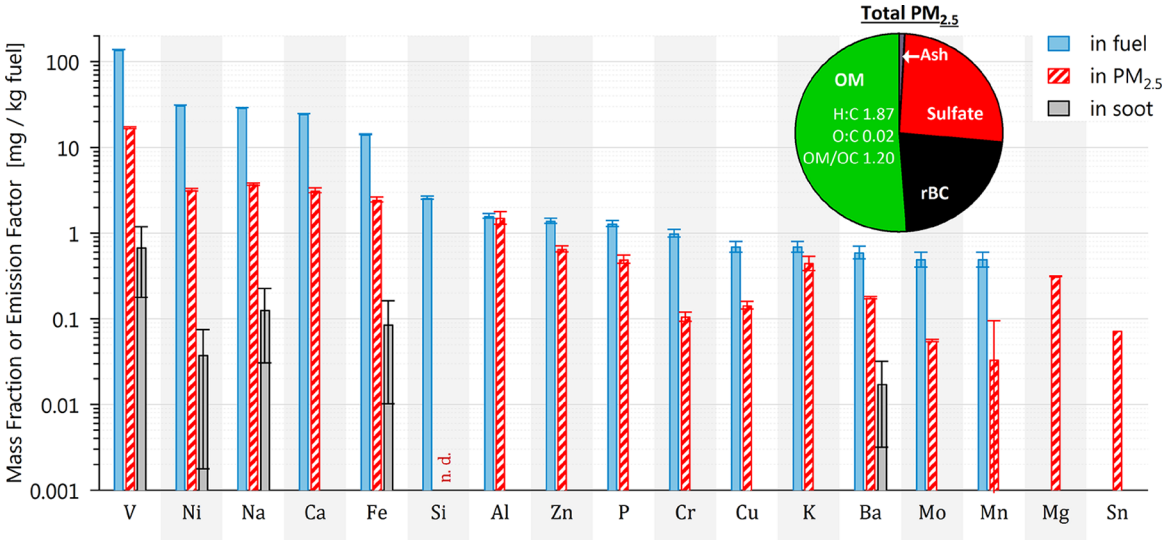

Figure 1. Trace-element composition of the fuel (mass fraction) and of the $PM_{2.5}$ and soot (emission factors). All elements except C, H, O, and S are shown. The inset pie chart shows the overall PM composition, including OM elemental composition. Uncertainties are standard errors of the mean (s.e.m.) for the PM samples and 10% for the fuel composition. Si in $PM_{2.5}$ was not determined (n.d.). Other missing bars correspond to below-LOD signals; LODs are given in the text and in Tables S2 and S3.

Calculated Quantities. The mass ratio of a given metal M to BC in $PM_{2.5}$ was calculated as

$$(\mathrm{M{:}BC})_{\text{in-PM}_{2.5}} = \frac{C_{\mathrm{M,ICP\text{-}OES}}}{C_{\mathrm{EC,PM_{2.5}}}} \quad (1)$$

where $C_{\mathrm{M,ICP\text{-}OES}}$ is the mass concentration of that metal M in the $PM_{2.5}$, and $C_{\mathrm{EC,PM_{2.5}}}$ is the EC mass concentration measured by the thermal–optical IMPROVE protocol after the $PM_{2.5}$ cyclone for the same filter, representing $C_{\mathrm{rBC,PM_{2.5}}}$, which previous studies have found to agree well with rBC mass concentrations.[52,65,67]

The mass ratio of a given metal M to rBC in soot particles was determined as

$$(\mathrm{M{:}BC})_{\text{in-soot}} = \frac{C_{\mathrm{M,SP\text{-}AMS}}}{C_{\mathrm{rBC,SP\text{-}AMS}}} \quad (2)$$

where $C_{\mathrm{M,SP\text{-}AMS}}$ and $C_{\mathrm{rBC,SP\text{-}AMS}}$ are the mass concentrations of metal M and of rBC measured by SP-AMS. We observe that the ratio $(\mathrm{M{:}BC})_{\text{in-soot}}$ is approximately equal to the mass fraction of the metal in soot, since $C_{\mathrm{M,SP\text{-}AMS}}$ was on the order of 1% and since the presence of nonrefractory material internally mixed with the measured soot particles was negligible, as shown elsewhere.[44] However, the discussion below is not dependent upon this observation.

Following from eq 2, the emission factor of a given metal M per mass of CO_2 is

$$\mathrm{EF_M} = \frac{C_{\mathrm{M}}}{C_{\mathrm{CO_2}}} = \frac{(\mathrm{M{:}BC})_{\text{in-soot}} C_{\mathrm{rBC,SP2}}}{C_{\mathrm{CO_2}}} \quad (3)$$

This equation uses $C_{\mathrm{rBC,SP2}}$ rather than $C_{\mathrm{rBC,SP\text{-}AMS}}$ or $C_{\mathrm{EC,PM_{2.5}}}$, respectively, because of the E_z issues noted above and because of the high time resolution of the SP2 relative to the thermal–optical analysis. Emission factors for other PM components were calculated similarly to eq 3, replacing C_{M} with the appropriate measurement.

Uncertainties. ICP-OES $PM_{2.5}$ uncertainties were calculated as the quadratic sum of the standard deviation of the background, and 5% of the signal of the latter is an estimated proportional error[68]. When averaging data to ICP-OES-filter-sampling periods, the standard error of the mean was used.

SP-AMS and AMS uncertainties were calculated by combining peak-integration uncertainties with ion-counting uncertainties.[69] Peak-integration uncertainties were obtained with an improved-efficiency implementation of the Monte Carlo calculations described by Corbin et al.[69] The peak-width uncertainty used was 3%. We estimate that the worst-case uncertainty of the metal RIEs reported by Carbone et al.[40] are on the order of ~20%.

SP2 calibration and particle-counting uncertainties were generally smaller than the engine variability, such that the standard error of a typical mean rBC mass concentration (representing temporal variability) was larger than the propagated statistical uncertainty. The SP2 correction factor for the mass fraction of rBC particles that were too large or too small to be quantified, described above, resulted in a correction factor for HFO of 1.46 ± 0.15, where 0.15 is the estimated day-to-day variability of the 1.46 correction factor.

RESULTS AND DISCUSSION

Overview of $PM_{2.5}$ Composition. The composition of the ship-engine HFO PM was dominated by OM, BC, and sulfates. Since ammonia and nitrate emission factors were negligible, we infer that the dominant sulfate species was sulfuric acid. The pie chart in Figure 1 shows the mean relative emission factors of OM, BC, sulfate, and ash for a typical engine load of 50%. Note that these emission factors reflect the composition of the primary particulate emissions of this engine and do not account for the formation of secondary sulfate and secondary OM, which may occur in the atmosphere on a time scale of hours for OM and days for sulfate. More details on these emission factors are given in Corbin et al.,[44] and the relationship between such emission factors and engine load has been discussed by Müller et al.[70] Ash is defined as all elements other than CHOS and was

DOI: 10.1021/acs.est.8b01764
Environ. Sci. Technol. 2018, 52, 6714–6722

measured by ICP-OES. Note that this definition excludes the oxygen contained in metal oxides.

The pie chart of Figure 1 also includes the OM to OC mass ratio (OM/OC) and the elemental ratios H/C and O/C, all from the high-resolution AMS data[55,56] (see the SI for details). The OM/OC, required to convert thermally evolved carbon measurements to total OM mass, was 1.2 on average. This is lower than the value of 1.6 recommended for urban aerosols by Turpin and Lim,[71] due to the near absence of oxygen in our OM (O/C 0.02 ± 0.02, H/C 1.87 ± 0.07).

Using SEM, we identified soot aggregates, spherical, tar-ball-like particles, and irregular ash particles in the HFO PM. No porous char cenospheres[45] were observed. This observation rules out the hypothesis that supermicron char particles, not detectable by SP-AMS due to their size, influenced our results. Applying SEM-EDX to 56 randomly chosen micron-sized particles, we detected Ca, S, Al, Zn, V, Si, and Ni in irregular combinations. This irregularity highlights the strength of the SP-AMS, which sampled ~10^5 particles per second, such that counting statistics are a negligible source of uncertainty. Obtaining a comparable SEM-EDX data set was infeasible for this study. We reiterate here that the SP-AMS methodology we have employed has been directly validated in the laboratory[40] and does not rely on the SEM for quantification.

Emission Factors of Trace Metals in Soot Particles. The trace-element compositions of the fuel (relative to the bulk mass) and $PM_{2.5}$ (as emission factors) are shown by the leftmost and central bars in Figure 1, respectively. These compositions were both measured by ICP-OES. Overall, HFO contained ~110 mg/kg of trace metals (with signals above LOD), whereas MGO and diesel contained negligible amounts (only Fe in MGO was above the general detection limit of 0.1 mg/kg, at 0.2 mg/kg). Trace elements in both the HFO fuel and PM were dominated by V, with Ni, Na, Ca, Fe, and other less-abundant species present. The relative presence of V and Ni is discussed further below. The ratio of fuel composition to emission factor for each element was ~2−10 in $PM_{2.5}$ and ~100 in soot (Figure 1, Figure S4).

The rightmost bars for each metal in Figure 1 show that the emission factors of metal inclusions in soot particles, as measured by the SP-AMS ("in-soot metals", eq 3), were much lower than for the $PM_{2.5}$. This is primarily because the $PM_{2.5}$ measurements additionally include externally mixed metal oxides and salts. V concentrations were a factor of 25 lower in soot than in the $PM_{2.5}$. For Ni, this factor was 84. Given that the rBC mass was a factor of four lower than the overall $PM_{2.5}$ mass (Figure 1), this translates to a relative depletion of metals in soot by about an order of magnitude, compared to the metals present in the overall $PM_{2.5}$. The error bars in Figure 1 indicate standard errors of the respective means. These were much larger for in-soot metals than for in-$PM_{2.5}$ metals, indicating a substantial variability in the internal mixing of soot with each metal. Note that this variability does not indicate noise in the SP-AMS data; it is much greater than the expected instrument precision (discussed in the SI). In addition, the metal-in-soot concentrations were not correlated with the total $PM_{2.5}$ metal concentrations (Figure S9), demonstrating the independence of these two quantities.

We note that the reported metal ions were generally atomic ions (M^+) of the respective metals, with two exceptions. First, a very small mass fraction of V (3.5%) was observed as VO^+ (see the SI and Table S5). Second, a more substantial mass fraction of Fe (12%) was observed as FeO^+ and Fe_2O^+. Oxide ions of all other reported metals were not present. This indicates that the metallic species present in our samples were either metallic compounds or oxides which thermally degraded upon heating.[72]

We did not observe metal-sulfate ions in the SP-AMS mass spectra, in spite of the presence of substantial amounts of sulfate mass in the PM (Figure 1). This is not a limitation of the SP-AMS. Carbone et al.[40] used an SP-AMS to measure VSO_x, $CaSO_x$, and $FeSO_x$ ions in PM generated by a heating station operated on an aqueous emulsion of HFO and distillate fuel. This difference between our results and those of Carbone et al. provides physical insight into the composition of HFO PM. In particular, since emulsions lead to lower combustion temperatures,[73] resulting in the preferential formation of metal sulfates rather than oxides,[18,32] the absence of metal sulfates in our mass spectra represents an indicator of combustion temperature. Our results therefore indicate that studies which use laboratory combustors[74,75] may produce PM which is not representative of the HFO PM produced by four-stroke marine diesel engines. Toxicological studies should therefore use ship engines[13] rather than boilers[12,76] to simulate marine pollution.

Metal to BC Mass Ratios in Soot and $PM_{2.5}$. The mass ratios of each quantified metal to BC are shown in Figure 2 for each metal where in-soot concentrations were quantified by SP-AMS. These ratios are shown for the specific cases of in-soot mass, $(M:BC)_{in\text{-}soot}$, and in-$PM_{2.5}$ mass $(M:BC)_{in\text{-}PM_{2.5}}$. The ratio $(M:BC)_{in\text{-}soot}$ was less than 0.03 in all cases, corresponding to a few percent or less mass contribution to the refractory mass of soot particles. For toxicology studies, this depletion means that only a small fraction of the metal mass is rendered biologically inaccessible by incorporation into soot particles.

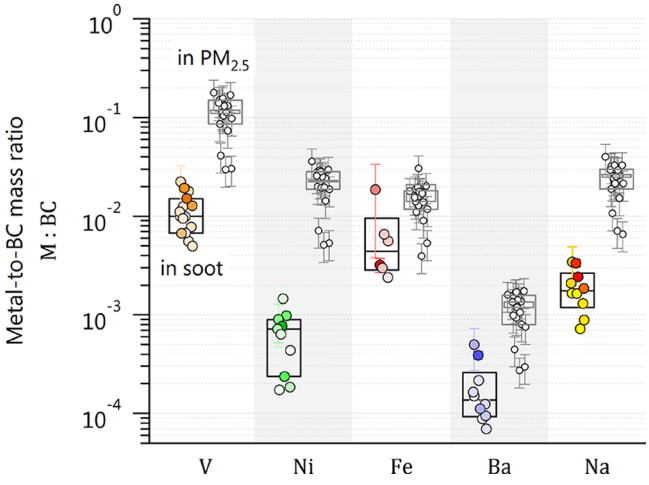

Figure 2. Metal:BC mass ratios in soot and in $PM_{2.5}$. The ratios were obtained from the in-soot and in-$PM_{2.5}$ metal concentrations (defined respectively by eq 2 and eq 1) in combination with the in-soot BC mass or all-$PM_{2.5}$ BC mass, as defined in those equations. For soot, the data points are colored darker for higher $C_{SP\text{-}AMS,M}$ concentrations. Fewer data points are plotted for soot due to limited availability of SP2 data. Boxes show 25−50−75th percentiles; error bars are s.e.m.

However, this small mass fraction may be sufficient to catalyze BC oxidation within the engine. Such BC oxidation is a major factor in determining the BC emissions of an engine, since the vast majority of BC produced by a flame is generally destroyed (oxidized) before leaving it.[42]

DOI: 10.1021/acs.est.8b01764
Environ. Sci. Technol. 2018, 52, 6714−6722

To evaluate this hypothesis, we compare our measured in-soot metal content to the data reported by Bladt et al.,[35] who observed a large change in temperature-programmed oxidation results for BC with 10 mass% of Fe and higher. Although those authors did not report measurements below 5 mass%, their reported exponential dependence of oxidation temperature on Fe mass% suggests that our observed few percent metal content may have a significant influence on BC emissions. We also note that in addition to BC oxidation, the presence of metals may influence BC formation.[36] These effects would mean that the soot emission factors of HFO are a function of the metal content of the fuel, which is expected to vary significantly between fuels.[77] Further study is required to establish whether this fuel-to-fuel variability is substantial in the context of engine-to-engine variation.

The high outlier for Fe in Figure 2 is noteworthy, suggesting that $(Fe:BC)_{in\text{-}soot}$ may have been externally mixed for this point. Uniquely to all other SP-AMS-quantified metals, this outlier corresponds to a period of measurement where $C_{SP\text{-}AMS,Fe}$ was poorly correlated with $C_{SP\text{-}AMS,rBC}$. We conclude that this point was likely biased high due to the anomalous presence of light-absorbing Fe or Fe compounds.

Enhanced Vanadium-to-Nickel Ratio in Soot. The ratio V:Ni has been recommended for the source apportionment of residual-fuel PM in atmospheric studies. In this section we examine whether this ratio changes between in-$PM_{2.5}$ and in-soot metals. Also, since metals are incorporated into soot particles by vaporization/condensation, the metal-in-soot ratios provide quantitative insights into the degree to which some metals may be enhanced in ship-exhaust $PM_{2.5}$ or $PM_{0.1}$ particles relative to coarse-mode PM.

Our $PM_{2.5}$ data (Figure 3) indicate a mean and standard deviation V:Ni of 5.2 ± 0.5. This ratio is comparable to those

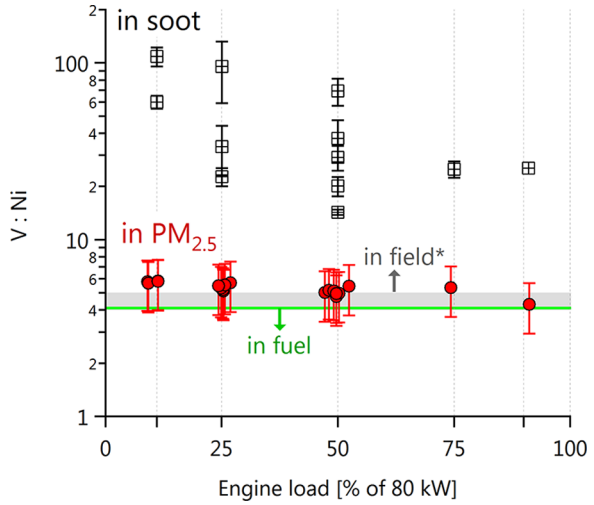

Figure 3. Mass ratio V:Ni in soot particles and in the $PM_{2.5}$ of HFO exhaust. Also shown are the ranges of values measured in the fuel itself (green thin line) and in field measurements of atmospheric particles (gray shading, measured by Viana et al.[78]). The horizontal scatter of the $PM_{2.5}$ data is added for clarity only. Error bars are s.e.m.

reported by two previous studies. Based on a source-apportionment analysis of atmospheric data, Viana et al.[78] suggested that a V:Ni of 4−5 is representative of HFO combustion. Consistent with this range of values, Agrawal et al.[79] observed a ratio of 4.5 ± 0.1 for an in-use ship. However, Lyyränen et al.[16] reported a lower ratio, close to unity, possibly due to a difference in fuel composition. Our $PM_{2.5}$ data do not show a dependence of V:Ni in $PM_{2.5}$ on the engine load, also consistent with Agrawal et al.[79]

Whereas V:Ni was similar between the fuel and the $PM_{2.5}$, V:Ni in soot particles was 20−100, which is 4- to 25-times higher than in the $PM_{2.5}$. This enhancement is well outside of the SP-AMS uncertainty range. Source apportionment studies based on SP-AMS or other laser-vaporization instruments with high sensitivities to BC, such as laser desorption/ionization,[5,7,80,81] will therefore measure different V:Ni ratios than ICP-OES or similar techniques. We note that the in-soot V:Ni appeared to increase at lower engine loads, in contrast to the in-$PM_{2.5}$ V:Ni. Additional measurements at high engine loads are needed in future studies to corroborate this potential trend.

We also attempted to measure the composition of micron-sized particles using SEM-EDX, for comparison with the bulk $PM_{2.5}$ and soot particles results. However, this method was of limited statistical power, as we found that sufficient amounts of V and Ni were present in only 3 of 56 measured particles. The V:Ni ratios of these particles was 2.44 ± 0.34, 1.07 ± 0.68, and 1.23 ± 0.28. This limited evidence suggests that the V:Ni ratio of supermicron particles more closely resembles that of $PM_{2.5}$ than that of soot.

When switching from HFO fuel to distillate fuels, we did not observe V or Ni in the emissions. Thus, the possibilities of V and Ni originating directly from the engine itself (e.g., via abrasion) as well as the interference of resuspended particles can be ruled out. Also, this shows that V:Ni is a specific tracer for HFO emissions and allows ship-exhaust to be identified only when HFO is the fuel. This presents a challenge to future ship-exhaust source apportionment studies, as HFO emissions must be minimized within SECAs.[82] We note that the use of exhaust scrubbers[83] can be used to accomplish this minimization and that exhaust scrubbers are least effective for the smallest size fraction.[26] Therefore, our observed enrichment of toxic vanadium in soot particles indicates a per-mass enhanced toxicity in scrubbed HFO exhaust.

Overall, we conclude that vanadium inclusions in soot were more likely to form than nickel inclusions. We compare this conclusion with the thermodynamical calculations of Sippula et al.,[18] which indicate that VO_2 should be the first species to nucleate in the engine, followed by iron and nickel (at 1200−1300 °C). Our observations are in agreement with these predictions.

Implications for HFO PM Toxicity. Since our observed enhancement of vanadium in soot particles was attributed to the higher-temperature condensation of vanadium in the engine compared to other metals, this enhancement is independent of the chemistry that leads to soot formation. Therefore, V is expected to be enhanced not only in soot particles but also in all small (diameters < 100 nm) particles emitted by HFO combustion in marine diesel engines. This would mean that the V:Ni relevant for source-apportionment of atmospheric PM to HFO particles may depend on the measured size fraction. Moreover, since vanadium is especially toxic,[27] and since the penetration of particles into the human lungs is size-dependent, with smaller particles penetrating deeper into the lungs and alveoli, this would correspond to an enhanced toxicity of smaller HFO particles due to their enhanced vanadium content. Although incorporation into soot particles would render this vanadium biologically inaccessible, we observed (above) that this effect sequesters <3% of the total $PM_{2.5}$ vanadium. Relevant

DOI: 10.1021/acs.est.8b01764
Environ. Sci. Technol. 2018, 52, 6714−6722

to this conclusion, we note that the translocation of insoluble PM into the blood and subsequent accumulation in organs is a strong function of particle size, being significantly enhanced for diameters below ~100 nm.[24] The temperature dependence of this small-particle enhancement in V also indicates that the toxicity of HFO PM is dependent on the combustion conditions, in particular on temperature, for a given fuel. When performing size-resolved PM exposures, size-resolved chemical composition determination is therefore essential.

■ ASSOCIATED CONTENT

Supporting Information

The Supporting Information is available free of charge on the ACS Publications website at DOI: 10.1021/acs.est.8b01764.

Additional information on the quantification of metals by ICP-OES and by SP-AMS; additional discussion of the SP-AMS rBC transmission efficiency; supplemental figures and tables (PDF)

■ AUTHOR INFORMATION

Corresponding Author

*E-mail: martin.gysel@psi.ch.

ORCID

J. C. Corbin: 0000-0002-2584-9137

H. Czech: 0000-0001-8377-4252

F. Buatier de Mongeot: 0000-0002-8144-701X

Present Addresses

‡J.C.C.: Measurement Science and Standards, National Research Council Canada, 1200 Montreal Road, Ottawa K1A 0R6, Canada.

#M.Z.: Alfred Wegener Institute, Am Handelshafen 12, 27570 Bremerhaven, Germany.

Author Contributions

J.C.C. analyzed the SP-AMS and SP2 data and drafted the manuscript. J.C.C., M.G., H.C., I.E.H., M.Z., and A.A.M. interpreted the data. M.Z., J.C.C., and M.G. operated and calibrated SP2. A.A.M. and S.M.P. operated and calibrated the SP-AMS with contributions from N.K.K. J.O., Y.H., and S.M.P. performed the filter sampling. B.M. performed the ICP-OES analysis, D.M., F.B.M., and C.M. performed the SEM-EDX analysis, and H.C. performed the NIOSH analysis. S.M.P., J.O., and B.S. oversaw the experiments, B.S. operated the engine, and A.S.H.P. and R.Z. initiated the study.

Notes

The authors declare no competing financial interest.

■ ACKNOWLEDGMENTS

This project, WOOSHI, was funded by the Swiss National Science Foundation (SNSF, project number 140590), the German Science Foundation (DFG, grant ZI 764/5-1), and the Helmholtz Virtual Institute "HICE – Aerosol and Health" (www.hice-vi.eu) via the Helmholtz Association (HGF-INF). J.C.C., M.Z., and M.G. were funded by the ERC under grant ERC-CoG-615922-BLACARAT.

■ REFERENCES

(1) Eyring, V.; Köhler, H.; Van Aardenne, J.; Lauer, A. Emissions from international shipping: 1. The last 50 years. *J. Geophys. Res.* **2005**, *110*, D17305.

(2) Eyring, V.; Isaksen, I. S.; Berntsen, T.; Collins, W. J.; Corbett, J. J.; Endresen, O.; Grainger, R. G.; Moldanova, J.; Schlager, H.; Stevenson, D. S. Transport impacts on atmosphere and climate: Shipping. *Atmos. Environ.* **2010**, *44*, 4735–4771.

(3) Corbett, J. J.; Winebrake, J. J.; Green, E. H.; Kasibhatla, P.; Eyring, V.; Lauer, A. Mortality from ship emissions: a global assessment. *Environ. Sci. Technol.* **2007**, *41*, 8512–8518.

(4) Global Trade Statistics, World Shipping Council, 2017. http://www.worldshipping.org/about-the-industry/global-trade/ (accessed 2017-08-29).

(5) Yau, P.; Lee, S.; Cheng, Y.; Huang, Y.; Lai, S.; Xu, X. Contribution of ship emissions to the fine particulate in the community near an international port in Hong Kong. *Atmos. Res.* **2013**, *124*, 61–72.

(6) Liu, H.; Fu, M.; Jin, X.; Shang, Y.; Shindell, D.; Faluvegi, G.; Shindell, C.; He, K. Health and climate impacts of ocean-going vessels in East Asia. *Nat. Clim. Change* **2016**, *6*, 1037–1041.

(7) Liu, Z.; Lu, X.; Feng, J.; Fan, Q.; Zhang, Y.; Yang, X. Influence of Ship Emissions on Urban Air Quality: A Comprehensive Study Using Highly Time-Resolved Online Measurements and Numerical Simulation in Shanghai. *Environ. Sci. Technol.* **2017**, *51*, 202–211.

(8) Laden, F.; Neas, L. M.; Dockery, D. W.; Schwartz, J. Association of fine particulate matter from different sources with daily mortality in six US cities. *Environ. Health Perspect.* **2000**, *108*, 941.

(9) Janssen, N. A.; Schwartz, J.; Zanobetti, A.; Suh, H. H. Air conditioning and source-specific particles as modifiers of the effect of PM (10) on hospital admissions for heart and lung disease. *Environ. Health Perspect.* **2002**, *110*, 43.

(10) Lighty, J. S.; Veranth, J. M.; Sarofim, A. F. Combustion aerosols: factors governing their size and composition and implications to human health. *J. Air Waste Manage. Assoc.* **2000**, *50*, 1565–1618.

(11) Wörle-Knirsch, J. M.; Kern, K.; Schleh, C.; Adelhelm, C.; Feldmann, C.; Krug, H. F. Nanoparticulate Vanadium Oxide Potentiated Vanadium Toxicity in Human Lung Cells. *Environ. Sci. Technol.* **2007**, *41*, 331–336.

(12) Kaivosoja, T.; Jalava, P.; Lamberg, H.; Virén, A.; Tapanainen, M.; Torvela, T.; Tapper, U.; Sippula, O.; Tissari, J.; Hillamo, R.; Hirvonen, M.-R.; Jokiniemi, J. Comparison of emissions and toxicological properties of fine particles from wood and oil boilers in small (20–25 kW) and medium (5–10 MW) scale. *Atmos. Environ.* **2013**, *77*, 193–201.

(13) Oeder, S.; et al. Particulate matter from both heavy fuel oil and diesel fuel shipping emissions show strong biological effects on human lung cells at realistic and comparable in vitro exposure conditions. *PLoS One* **2015**, *10*, e0126536.

(14) Sapcariu, S. C.; et al. Metabolic Profiling as Well as Stable Isotope Assisted Metabolic and Proteomic Analysis of RAW 264.7 Macrophages Exposed to Ship Engine Aerosol Emissions: Different Effects of Heavy Fuel Oil and Refined Diesel Fuel. *PLoS One* **2016**, *11*, e0157964.

(15) Miller, C.; Linak, W.; King, C.; Wendt, J. Fine Particle Emissions from Heavy Fuel Oil Combustion in a Firetube Package Boiler. *Combust. Sci. Technol.* **1998**, *134*, 477–502.

(16) Lyyränen, J.; Jokiniemi, J.; Kauppinen, E. I.; Joutsensaari, J. Aerosol characterisation in medium-speed diesel engines operating with heavy fuel oils. *J. Aerosol Sci.* **1999**, *30*, 771–784.

(17) Fridell, E.; Steen, E.; Peterson, K. Primary particles in ship emissions. *Atmos. Environ.* **2008**, *42*, 1160–1168.

(18) Sippula, O.; Hokkinen, J.; Puustinen, H.; Yli-Pirilä, P.; Jokiniemi, J. Comparison of particle emissions from small heavy fuel oil and wood-fired boilers. *Atmos. Environ.* **2009**, *43*, 4855–4864.

(19) Moldanová, J.; Fridell, E.; Popovicheva, O.; Demirdjian, B.; Tishkova, V.; Faccinetto, A.; Focsa, C. Characterisation of particulate matter and gaseous emissions from a large ship diesel engine. *Atmos. Environ.* **2009**, *43*, 2632–2641.

(20) Hofmann, W. Modelling inhaled particle deposition in the human lung—A review. *J. Aerosol Sci.* **2011**, *42*, 693–724.

(21) Wiebert, P.; Sanchez-Crespo, A.; Falk, R.; Philipson, K.; Lundin, A.; Larsson, S.; Möller, W.; Kreyling, W. G.; Svartengren, M. No Significant Translocation of Inhaled 35-nm Carbon Particles to the Circulation in Humans. *Inhalation Toxicol.* **2006**, *18*, 741–747.

(22) Wiebert, P.; Sanchez-Crespo, A.; Seitz, J.; Falk, R.; Philipson, K.; Kreyling, W.; Möller, W.; Sommerer, K.; Larsson, S.; Svartengren, M. Negligible clearance of ultrafine particles retained in healthy and affected human lungs. *Eur. Respir. J.* **2006**, *28*, 286−290.
(23) Kreyling, W. G.; Semmler-Behnke, M.; Möller, W. Ultrafine Particle−Lung Interactions: Does Size Matter? *J. Aerosol Med.* **2006**, *19*, 74−83.
(24) Geiser, M.; Kreyling, W. G. Deposition and biokinetics of inhaled nanoparticles. *Part. Fibre Toxicol.* **2010**, *7*, 2.
(25) Ghio, A. J. Metals associated with both the water-soluble and -insoluble fractions of an ambient air pollution particle catalyze and oxidative stress. *Inhalation Toxicol.* **1999**, *11*, 37−49.
(26) Shendrikar, A.; Ensor, D.; Cowen, S.; Woffinden, G.; McElroy, M. Size-dependent penetration of trace elements through a utility baghouse. *Atmos. Environ. (1967-1989)* **1983**, *17*, 1411−1421.
(27) Thompson, K. H.; Orvig, C. Boon and Bane of Metal Ions in Medicine. *Science* **2003**, *300*, 936−939.
(28) Speight, J. G. *The desulfurization of heavy oils and residual fuel*; CRC Press: 1999.
(29) Czernuszewicz, R. S. Geochemistry of porphyrins: biological, industrial and environmental aspects. *J. Porphyrins Phthalocyanines* **2000**, *04*, 426−431.
(30) Caumette, G.; Lienemann, C.-P.; Merdrignac, I.; Bouyssiere, B.; Lobinski, R. Element speciation analysis of petroleum and related materials. *J. Anal. At. Spectrom.* **2009**, *24*, 263−276.
(31) Kasper, M.; Sattler, K.; Siegmann, K.; Matter, U.; Siegmann, H. The influence of fuel additives on the formation of carbon during combustion. *J. Aerosol Sci.* **1999**, *30*, 217−225.
(32) Linak, W. P.; Miller, C. A.; Wendt, J. O. Fine particle emissions from residual fuel oil combustion: Characterization and mechanisms of formation. *Proc. Combust. Inst.* **2000**, *28*, 2651−2658.
(33) Popovicheva, O.; Kireeva, E.; Shonija, N.; Zubareva, N.; Persiantseva, N.; Tishkova, V.; Demirdjian, B.; Moldanová, J.; Mogilnikov, V. Ship particulate pollutants: Characterization in terms of environmental implication. *J. Environ. Monit.* **2009**, *11*, 2077−2086.
(34) Streibel, T.; et al. Aerosol emissions of a ship diesel engine operated with diesel fuel or heavy fuel oil. *Environ. Sci. Pollut. Res.* **2017**, *24*, 10976.
(35) Bladt, H.; Schmid, J.; Kireeva, E. D.; Popovicheva, O. B.; Perseantseva, N. M.; Timofeev, M. A.; Heister, K.; Uihlein, J.; Ivleva, N. P.; Niessner, R. Impact of Fe Content in Laboratory-Produced Soot Aerosol on its Composition, Structure, and Thermo-Chemical Properties. *Aerosol Sci. Technol.* **2012**, *46*, 1337−1348.
(36) Simonsson, J.; Olofsson, N.-E.; Bladh, H.; Sanati, M.; Bengtsson, P.-E. Influence of potassium and iron chloride on the early stages of soot formation studied using imaging LII/ELS and TEM techniques. *Proc. Combust. Inst.* **2017**, *36*, 853−860.
(37) Onasch, T. B.; Trimborn, A.; Fortner, E. C.; Jayne, J. T.; Kok, G. L.; Williams, L. R.; Davidovits, P.; Worsnop, D. R. Soot Particle Aerosol Mass Spectrometer: Development, Validation, and Initial Application. *Aerosol Sci. Technol.* **2012**, *46*, 804−817.
(38) Schwarz, J. P.; et al. Single-particle measurements of midlatitude black carbon and light-scattering aerosols from the boundary layer to the lower stratosphere. *J. Geophys. Res.* **2006**, *111*, D16207.
(39) Corbin, J. C.; Sierau, B.; Gysel, M.; Laborde, M.; Keller, A.; Kim, J.; Petzold, A.; Onasch, T. B.; Lohmann, U.; Mensah, A. A. Mass spectrometry of refractory black carbon particles from six sources: carbon-cluster and oxygenated ions. *Atmos. Chem. Phys.* **2014**, *14*, 2591−2603.
(40) Carbone, S.; Onasch, T.; Saarikoski, S.; Timonen, H.; Saarnio, K.; Sueper, D.; Rönkkö, T.; Pirjola, L.; Häyrinen, A.; Worsnop, D.; Hillamo, R. Characterization of trace metals on soot aerosol particles with the SP-AMS: detection and quantification. *Atmos. Meas. Tech.* **2015**, *8*, 4803−4815.
(41) Canagaratna, M.; et al. Chemical and microphysical characterization of ambient aerosols with the aerodyne aerosol mass spectrometer. *Mass Spectrom. Rev.* **2007**, *26*, 185−222.
(42) Glassman, I.; Yetter, R. A. *Combustion*; Academic Press: Burlington, MA, USA, 2008.
(43) Petzold, A.; Ogren, J.; Fiebig, M.; Laj, P.; Li, S.-M.; Baltensperger, U.; Holzer-Popp, T.; Kinne, S.; Pappalardo, G.; Sugimoto, N.; Wehrli, C.; Wiedensohler, A.; Zhang, X.-Y. Recommendations for the interpretation of "black carbon" measurements. *Atmos. Chem. Phys.* **2013**, *13*, 8365−8379.
(44) Corbin, J. C.; Pieber, S. M.; Czech, H.; Zanatta, M.; Jakobi, G.; Massabò, D.; Orasche, J.; El Haddad, I.; Mensah, A. A.; Stengel, B.; Drinovec, L.; Močnik, G.; Zimmermann, R.; Prévôt, A. S. H.; Gysel, M. Brown and black carbon emitted by a marine engine operated on heavy fuel oil and distillate fuels: optical properties, size distributions, emission factors. 2018, manuscript in press at *Journal of Geophysical Research (Atmospheres)*, DOI: 10.1029/2017JD027818.
(45) Chen, Y.; Shah, N.; Braun, A.; Huggins, F. E.; Huffman, G. P. Electron microscopy investigation of carbonaceous particulate matter generated by combustion of fossil fuels. *Energy Fuels* **2005**, *19*, 1644−1651.
(46) Lyyränen, J.; Jokiniemi, J.; Kauppinen, E. I.; Backman, U.; Vesala, H. Comparison of Different Dilution Methods for Measuring Diesel Particle Emissions. *Aerosol Sci. Technol.* **2004**, *38*, 12−23.
(47) Sippula, O.; Koponen, T.; Jokiniemi, J. Behavior of Alkali Metal Aerosol in a High-Temperature Porous Tube Sampling Probe. *Aerosol Sci. Technol.* **2012**, *46*, 1151−1162.
(48) Chow, J. C.; Watson, J. G.; Chen, L.-W. A.; Chang, M. O.; Robinson, N. F.; Trimble, D.; Kohl, S. The IMPROVE_A Temperature Protocol for Thermal/Optical Carbon Analysis: Maintaining Consistency with a Long-Term Database. *J. Air Waste Manage. Assoc.* **2007**, *57*, 1014−1023.
(49) Stephens, M.; Turner, N.; Sandberg, J. Particle identification by laser-induced incandescence in a solid-state laser cavity. *Appl. Opt.* **2003**, *42*, 3726−3736.
(50) Park, K.; Kittelson, D. B.; Zachariah, M. R.; McMurry, P. H. Measurement of inherent material density of nanoparticle agglomerates. *J. Nanopart. Res.* **2004**, *6*, 267−272.
(51) Laborde, M.; et al. Single Particle Soot Photometer intercomparison at the AIDA chamber. *Atmos. Meas. Tech.* **2012**, *5*, 3077−3097.
(52) Laborde, M.; Mertes, P.; Zieger, P.; Dommen, J.; Baltensperger, U.; Gysel, M. Sensitivity of the Single Particle Soot Photometer to different black carbon types. *Atmos. Meas. Tech.* **2012**, *5*, 1031−1043.
(53) Canagaratna, M. R.; Massoli, P.; Browne, E. C.; Franklin, J. P.; Wilson, K. R.; Onasch, T. B.; Kirchstetter, T. W.; Fortner, E. C.; Kolb, C. E.; Jayne, J. T.; Kroll, J. H.; Worsnop, D. R. Chemical Compositions of Black Carbon Particle Cores and Coatings via Soot Particle Aerosol Mass Spectrometry with Photoionization and Electron Ionization. *J. Phys. Chem. A* **2015**, *119*, 4589−4599.
(54) Corbin, J. C.; Keller, A.; Sierau, B.; Lohmann, U.; Mensah, A. A. Black-carbon-surface oxidation and organic composition of beechwood soot aerosols. *Atmos. Chem. Phys.* **2015**, *15*, 11885−11907.
(55) Aiken, A. C.; DeCarlo, P. F.; Jimenez, J. L. Elemental analysis of organic species with electron ionization high-resolution mass spectrometry. *Anal. Chem.* **2007**, *79*, 8350−8358.
(56) Aiken, A. C.; DeCarlo, P. F.; Kroll, J. H.; Worsnop, D. R.; Huffman, J. A.; Docherty, K. S.; Ulbrich, I. M.; Mohr, C.; Kimmel, J. R.; Sueper, D. O/C and OM/OC ratios of primary, secondary, and ambient organic aerosols with high-resolution time-of-flight aerosol mass spectrometry. *Environ. Sci. Technol.* **2008**, *42*, 4478−4485.
(57) Canagaratna, M.; Jimenez, J.; Kroll, J.; Chen, Q.; Kessler, S.; Massoli, P.; Hildebrandt Ruiz, L.; Fortner, E.; Williams, L.; Wilson, K.; Surratt, J.; Donahue, N.; Jayne, J.; Worsnop, D. R. Elemental ratio measurements of organic compounds using aerosol mass spectrometry: characterization, improved calibration, and implications. *Atmos. Chem. Phys.* **2015**, *15*, 253−272.
(58) Jimenez, J. L.; Canagaratna, M. R.; Drewnick, F.; Allan, J. D.; Alfarra, M. R.; Middlebrook, A. M.; Slowik, J. G.; Zhang, Q.; Coe, H.; Jayne, J. T.; Worsnop, D. R. Comment on "The effects of molecular weight and thermal decomposition on the sensitivity of a thermal desorption aerosol mass spectrometer. *Aerosol Sci. Technol.* **2016**, *50*, i−xv.

DOI: 10.1021/acs.est.8b01764
Environ. Sci. Technol. 2018, 52, 6714−6722

(59) Sueper, D.; Jimenez, J. L.; Aiken, A.; DeCarlo, P. PIKA ToF-AMS High Resolution Analysis Software; 2011. cires.colorado.edu/jimenez-group/ToFAMSResources/ToFSoftware/PikaInfo (accessed October 2015).
(60) Onasch, T. B.; Fortner, E. C.; Trimborn, A. M.; Lambe, A. T.; Tiwari, A. J.; Marr, L. C.; Corbin, J. C.; Mensah, A. A.; Williams, L. R.; Davidovits, P.; Worsnop, D. R. Investigations of SP-AMS Carbon Ion Distributions as a Function of Refractory Black Carbon Particle Types. *Aerosol Sci. Technol.* **2015**, *49*, 409−422.
(61) Corbin, J. Mass Spectrometry of Atmospherically-Relevant Soot and Black-Carbon Particles. Ph.D. thesis, ETH Zurich, 2014; DOI: 10.3929/ethz-a-010402210.
(62) Slowik, J. G.; Cross, E. S.; Han, J.-H.; Kolucki, J.; Davidovits, P.; Williams, L. R.; Onasch, T. B.; Jayne, J. T.; Kolb, C. E.; Worsnop, D. R. Measurements of morphology changes of fractal soot particles using coating and denuding experiments: Implications for optical absorption and atmospheric lifetime. *Aerosol Sci. Technol.* **2007**, *41*, 734−750.
(63) Willis, M. D.; Lee, A. K. Y.; Onasch, T. B.; Fortner, E. C.; Williams, L. R.; Lambe, A. T.; Worsnop, D. R.; Abbatt, J. P. D. Collection efficiency of the Soot-Particle Aerosol Mass Spectrometer (SP-AMS) for internally mixed particulate black carbon. *Atmos. Meas. Tech.* **2014**, *7*, 4507−4516.
(64) Ahern, A. T.; Subramanian, R.; Saliba, G.; Lipsky, E. M.; Donahue, N. M.; Sullivan, R. C. Effect of secondary organic aerosol coating thickness on the real-time detection and characterization of biomass-burning soot by two particle mass spectrometers. *Atmos. Meas. Tech.* **2016**, *9*, 6117.
(65) Slowik, J. G.; et al. An Inter-Comparison of Instruments Measuring Black Carbon Content of Soot Particles. *Aerosol Sci. Technol.* **2007**, *41*, 295−314.
(66) Moteki, N.; Kondo, Y. Effects of Mixing State on Black Carbon Measurements by Laser-Induced Incandescence. *Aerosol Sci. Technol.* **2007**, *41*, 398−417.
(67) Kondo, Y.; Sahu, L.; Moteki, N.; Khan, F.; Takegawa, N.; Liu, X.; Koike, M.; Miyakawa, T. Consistency and Traceability of Black Carbon Measurements Made by Laser-Induced Incandescence, Thermal-Optical Transmittance, and Filter-Based Photo-Absorption Techniques. *Aerosol Sci. Technol.* **2011**, *45*, 295−312.
(68) Rocke, D. M.; Lorenzato, S. A two-component model for measurement error in analytical chemistry. *Technometrics* **1995**, *37*, 176−184.
(69) Corbin, J. C.; Othman, A.; Allan, J. D.; Worsnop, D. R.; Haskins, J. D.; Sierau, B.; Lohmann, U.; Mensah, A. A. Peak-fitting and integration imprecision in the Aerodyne aerosol mass spectrometer: effects of mass accuracy on location-constrained fits. *Atmos. Meas. Tech.* **2015**, *8*, 4615−4636.
(70) Mueller, L.; et al. Characteristics and temporal evolution of particulate emissions from a ship diesel engine. *Appl. Energy* **2015**, *155*, 204−217.
(71) Turpin, B. J.; Lim, H.-J. Species contributions to PM2.5 mass concentrations: Revisiting common assumptions for estimating organic mass. *Aerosol Sci. Technol.* **2001**, *35*, 602−610.
(72) Quann, R.; Sarofim, A. Vaporization of refractory oxides during pulverized coal combustion. *Symp. (Int.) Combust., [Proc.]* **1982**, *19*, 1429−1440.
(73) Ballester, J. M.; Fueyo, N.; Dopazo, C. Combustion characteristics of heavy oil-water emulsions. *Fuel* **1996**, *75*, 695−705.
(74) Huffman, G. P.; Huggins, F. E.; Shah, N.; Huggins, R.; Linak, W. P.; Miller, C. A.; Pugmire, R. J.; Meuzelaar, H. L.; Seehra, M. S.; Manivannan, A. Characterization of Fine Particulate Matter Produced by Combustion of Residual Fuel Oil. *J. Air Waste Manage. Assoc.* **2000**, *50*, 1106−1114.
(75) Pattanaik, S.; Huggins, F. E.; Huffman, G. P. Chemical Speciation of Fe and Ni in Residual Oil Fly Ash Fine Particulate Matter Using X-ray Absorption Spectroscopy. *Environ. Sci. Technol.* **2012**, *46*, 12927−12935.
(76) Silbajoris, R.; Ghio, A. J.; Sanet, J. M.; Jaskot, R.; Dreher, K. L.; Brighton, L. E. In vivo and in vitro correlation of pulmonary map kinase activation following metallic exposure. *Inhalation Toxicol.* **2000**, *12*, 453−468.
(77) Stout, S.; Wang, Z. *Standard Handbook Oil Spill Environmental Forensics: Fingerprinting and Source Identification*; Academic Press: 2016; pp 641−683.
(78) Viana, M.; Amato, F.; Alastuey, A.; Querol, X.; Moreno, T.; García Dos Santos, S.; Herce, M. D.; Fernández-Patier, R. Chemical tracers of particulate emissions from commercial shipping. *Environ. Sci. Technol.* **2009**, *43*, 7472−7477.
(79) Agrawal, H.; Malloy, Q. G.; Welch, W. A.; Miller, J. W.; Cocker, D. R. In-use gaseous and particulate matter emissions from a modern ocean going container vessel. *Atmos. Environ.* **2008**, *42*, 5504−5510.
(80) Healy, R.; Hellebust, S.; Kourtchev, I.; Allanic, A.; O'Connor, I.; Bell, J.; Healy, D.; Sodeau, J.; Wenger, J. Source apportionment of PM 2.5 in Cork Harbour, Ireland using a combination of single particle mass spectrometry and quantitative semi-continuous measurements. *Atmos. Chem. Phys.* **2010**, *10*, 9593−9613.
(81) Ault, A. P.; Gaston, C. J.; Wang, Y.; Dominguez, G.; Thiemens, M. H.; Prather, K. A. Characterization of the Single Particle Mixing State of Individual Ship Plume Events Measured at the Port of Los Angeles. *Environ. Sci. Technol.* **2010**, *44*, 1954−1961.
(82) Czech, H.; Schnelle-Kreis, J.; Streibel, T.; Zimmermann, R. New directions: Beyond sulphur, vanadium and nickel − About source apportionment of ship emissions in emission control areas. *Atmos. Environ.* **2017**, *163*, 190−191.
(83) Lack, D. A.; Corbett, J. J. Black carbon from ships: a review of the effects of ship speed, fuel quality and exhaust gas scrubbing. *Atmos. Chem. Phys.* **2012**, *12*, 3985−4000.

DOI: 10.1021/acs.est.8b01764
Environ. Sci. Technol. 2018, 52, 6714−6722